Cell, Vol. 83, 301–311, October 20, 1995, Copyright © 1995 by Cell Press

Multiple Defects in the Immune System of *Lyn*-Deficient Mice, Culminating in Autoimmune Disease

Margaret L. Hibbs,* David M. Tarlinton,† Jane Armes,‡ Dianne Grail,* George Hodgson,* Rosemarie Maglitto,* Steven A. Stacker,* and Ashley R. Dunn*
*Ludwig Institute for Cancer Research
Melbourne Tumour Biology Branch
Royal Melbourne Hospital
Victoria 3050
Australia
†Walter and Eliza Hall Institute of Medical Research
Royal Melbourne Hospital
Victoria 3050
Australia
‡Department of Anatomical Pathology
Austin Hospital
Studley Road
Heidelberg, Victoria 3084
Australia

Summary

Mice homozygous for a disruption at the *Lyn* locus display abnormalities associated with the B lymphocyte lineage and in mast cell function. Despite reduced numbers of recirculating B lymphocytes, $Lyn^{-/-}$ mice are immunoglobulin M (IgM) hyperglobulinemic. Immune responses to T-independent and T-dependent antigens are affected. $Lyn^{-/-}$ mice fail to mediate an allergic response to IgE cross-linking, indicating that activation of LYN plays an indispensable role in FcεRI signaling. $Lyn^{-/-}$ mice have circulating autoreactive antibodies, and many show severe glomerulonephritis caused by the deposition of IgG immune complexes in the kidney, a pathology reminiscent of systemic lupus erythematosus. Collectively, these results implicate LYN as having an indispensable role in immunoglobulin-mediated signaling, particularly in establishing B cell tolerance.

Introduction

The SRC family of protein tyrosine kinases have been implicated in cell signaling through their physical association with different cell surface receptors that lack intrinsic catalytic activity (Bolen et al., 1992). Like several other members of the SRC family, LYN is expressed in a broad range of cell types and tissues (Bolen et al., 1992). Largely through coprecipitation studies, LYN has been shown to be physically associated with a number of hematopoietic cell surface receptors, including the B cell antigen receptor (BCR) (Yamanashi et al., 1991; Burkhardt et al., 1991; Campbell and Sefton, 1992), CD40 (Ren et al., 1994), the lipopolysaccharide (LPS) receptor (Stefanova et al., 1993), the high affinity FcεRI complex (Eiseman and Bolen, 1992), and the granulocyte colony-stimulating factor (G-CSF) receptor (Corey et al., 1994). In most cases, more than one member of the SRC family has been found to be associated with the same cell surface receptor, raising the possibility of functional redundancy within the SRC family, a notion supported by the milder than expected phenotype associated with mice in which one or other SRC-related kinase genes has been disrupted by homologous recombination in embryonic stem (ES) cells (reviewed by Varmus and Lowell, 1994).

A competent, signal-transducing BCR consists of an antigen-binding membrane immunoglobulin noncovalently associated with disulphide-linked heterodimers of immunoglobulin α and β/γ (Igα and Igβ/γ) subunits (Reth, 1992). While molecules that make up this BCR complex lack intrinsic catalytic activity, stimulation of resting B cells with antibodies to membrane immunoglobulin induces rapid tyrosine phosphorylation of B cell proteins, suggesting associated tyrosine kinase activities (Gold et al., 1990, 1991; Campbell and Sefton, 1990). This increase in total cellular tyrosine phosphorylation is correlated with an increase in the enzymatic activity of several members of the SRC family, including LYN, BLK, FYN, and FGR; indeed, coimmunoprecipitation studies have shown a physical association between the BCR complex and several members of the SRC family (Yamanashi et al., 1991; Burkhardt et al., 1991; Campbell and Sefton, 1992; Wechsler and Monroe, 1995). A highly conserved motif, termed the immunoreceptor tyrosine-based activation motif (ITAM), is found in many signal-transducing subunits including the cytoplasmic domain of the Igα and Igβ/γ molecules. Conserved tyrosine residues within this ITAM are a target for phosphorylation upon ligation of the BCR and presumably provide docking sites for additional molecules involved in B cell signaling, such as phosphatidylinositol 3-kinase, phospholipase C-γ2, and GTPase-activating protein. Recent studies have shown that the cytoplasmic domain of the Igα chain is constitutively associated with the SRC family kinases LYN and FYN (Clark et al., 1992; Pleiman et al., 1994a), suggesting that members of the SRC family may directly phosphorylate the ITAMs and, thus, participate in very early events in the BCR signal transduction cascade.

Signaling events from the BCR resemble those thus far characterized for the FcεRI complex (Ravetch, 1994). FcεRI is a tetrameric structure consisting of a ligand-binding α subunit, a β subunit, and homodimeric γ subunits (Blank et al., 1989). Like the Igα and Igβ/γ signaling molecules of the BCR complex, the cytoplasmic domains of the β and γ subunits of FcεRI also contain ITAMs (Ravetch, 1994). Biochemical studies have shown that LYN is associated with the β subunit, and it is thought that, on FcεRI triggering, LYN becomes activated and phosphorylates critical tyrosine residues in the ITAMs of both the β and γ subunits; the phosphorylation of γ recruits and activates $p72^{syk}$, which subsequently activates other molecules involved in the signal transduction cascade (reviewed by Ravetch, 1994).

To gain an insight into the physiological role of LYN and to gauge its importance in relaying signals from these

different cell surface receptors, we have generated *Lyn*$^{-/-}$ mice by gene targeting in ES cells. Our results show that LYN is an indispensable component of the BCR and FcεRI complexes and that its actions are required for the elimination of autoreactive antibodies.

Results

Derivation of *Lyn*$^{-/-}$ Mice

Initial attempts to create *Lyn*$^{-/-}$ mice were frustrated by the discovery that a significant portion of the coding sequences of the *Lyn* gene are duplicated (Hibbs et al., 1995). To overcome this problem, we constructed a targeting vector designed to replace the *Lyn* promoter and associated regulatory sequences with a PGKNeo expression cassette (Figure 1A). Following electroporation of the targeting construct into E14 ES cells, a polymerase chain reaction (PCR)-based screening assay was employed to screen 720 pools. DNA from two pools generated a PCR product whose size was predicted following homologous recombination of the targeting vector and the *Lyn* gene. On the basis of Southern blot analysis using a probe corresponding to sequences external to the targeting construct as well as a *neo* probe (data not shown), two clones, designated Lyn20.4 and Lyn81.1, were established. Following injection of targeted ES cells into C57BL/6 blastocysts, chimeras were generated, although only Lyn81.1 cells transmitted the disrupted *Lyn* locus through the germline. *Lyn*$^{+/-}$ animals were interbred to produce litters that included *Lyn*$^{-/-}$ offspring. Southern blot analysis of mouse tail DNA from progeny derived from such a mating identified the expected three genotypes (Figure 1B), and these were in a ratio consistent with normal patterns of Mendelian inheritance (158 *Lyn*$^{+/+}$, 292 *Lyn*$^{+/-}$, 130 *Lyn*$^{-/-}$). Mutant mice were viable and fertile, and young mice were superficially healthy.

To verify that the targeted *Lyn* gene was not expressed, reverse transcription–PCR (RT–PCR) analysis using *Lyn*-specific oligonucleotide primers (Hibbs et al., 1995) was undertaken with RNA derived from mouse livers. The expected 495 bp *Lyn*-related PCR product was only generated using RNA originating from *Lyn*$^{+/+}$ and *Lyn*$^{+/-}$ mice (data not shown). Moreover, while we were able to detect LYN autokinase activity in spleen and liver extracts from *Lyn*$^{+/+}$ and *Lyn*$^{+/-}$ animals, none was detected in extracts prepared from *Lyn*$^{-/-}$ animals (Figure 1C).

Lyn$^{-/-}$ Mice Have Reduced Numbers of Recirculating B Cells

The only discernible effect of the *Lyn* null mutation on leukocyte development was observed in the B lymphocyte lineage. Changes in the B cell lineage were investigated by flow cytometric analyses of lymphoid tissues using monoclonal antibodies (MAbs) to the pan-B cell marker B220 in combination with an array of MAbs specific for developmentally regulated markers. The profiles of *Lyn*$^{+/-}$ mice and *Lyn*$^{+/+}$ mice were indistinguishable (data not shown). The size of the pro-B (B220^{lo}/CD43^{+}/IgM^{-}), pre-B (B220^{lo}/CD43^{-}/IgM^{-}), and immature B (B220^{lo}/CD43^{-}/IgM^{+}) cell populations were the same in *Lyn*$^{+/+}$ and *Lyn*$^{-/-}$ bone marrow. The recirculating B cell (B220^{hi}/CD43^{-}/IgM^{+}) population in *Lyn*$^{-/-}$ bone marrow, however, was reduced by between 50% and 100% compared with controls (Figure 2). A reduction in the total number of B220^{+}/IgM^{+} cells was also observed in secondary lymphoid tissues from the *Lyn*$^{-/-}$ mice (Figures 2A and 2B), although again some

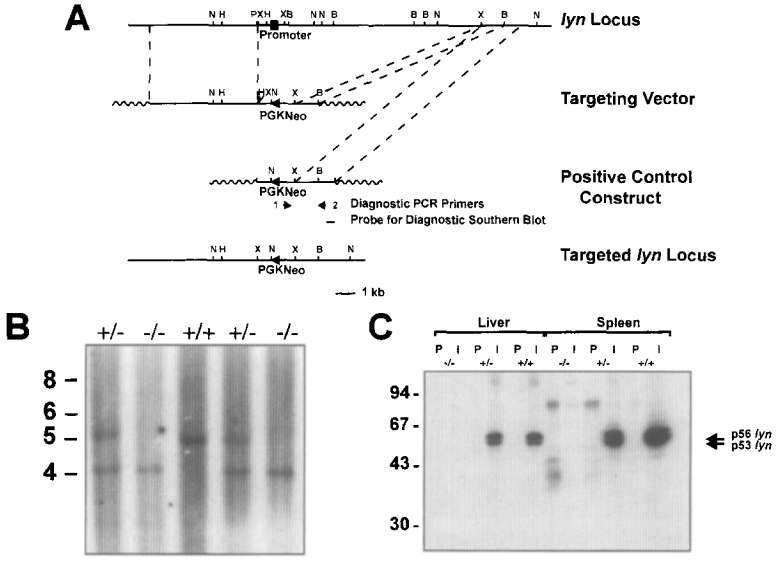

Figure 1. Generation of *Lyn*$^{-/-}$ Mice

(A) Targeting vector and homologous recombination at the *Lyn* locus. Shown is a partial restriction map of a portion of the *Lyn* locus; the closed box represents the mouse *Lyn* promoter. The targeting vector was constructed by replacing approximately 11.5 kb of genomic sequence with the PGKNeo expression cassette. The arrow represents the direction of transcription of PGKNeo. A positive control construct was generated by ligating an additional 840 bp of genomic sequence to the 3′ end of the short arm of the targeting construct and was used to develop a diagnostic PCR. The locations of diagnostic PCR primers 1 and 2 and the probe used for Southern blot analysis are indicated. Wavy lines indicate plasmid sequences. The predicted map of the mutated *Lyn* allele is shown at the bottom. B, BamHI; N, NcoI; H, HindIII; P, PstI; X, XbaI. Not all PstI sites are indicated.

(B) Representative Southern blot analysis of progeny from a heterozygote cross. Tail DNA was digested with NcoI and probed with the diagnostic probe shown in (A). The genotype of each animal is shown above the corresponding lane and is +/+, (wild type), +/− (heterozygote), and −/− (homozygous mutant). The size in kilobases is indicated on the left.

(C) Immunoprecipitation and kinase assay on liver and spleen extracts of *Lyn*$^{+/+}$, *Lyn*$^{+/-}$, and *Lyn*$^{-/-}$ mice. Extracts were immunoprecipitated with either preimmune sera (P) or anti-Lyn antisera (I) and subject to kinase assay. Phosphorylated products were separated on 10% polyacrylamide gels and revealed by autoradiography. The extracts were not equated for protein concentration. The relative molecular weight in kilodaltons is indicated on the left.

variation between mice and, somewhat surprisingly, between tissues was noted. Mesenteric lymph nodes always showed a greater reduction of B cells than the spleen and other lymph nodes from the same animal (Figures 2A and 2B). Intriguingly, lymph nodes from the axilla (Figures 2A and 2B) and groin (data not shown) showed a less pronounced reduction in B cells, possibly reflecting the extent to which the organs are activated. While there was also a reduction in B cells in the peripheral blood of $Lyn^{-/-}$ mice, this was not statistically significant (Figures 2A and 2B). Conventional B cells (B2), but not Ly-1$^+$ B cells (B1a), were markedly reduced in the peritoneal cavity of $Lyn^{-/-}$ mice (Figure 2B). The Peyer's patches in $Lyn^{-/-}$ mice were considerably smaller and in some instances undetectable macroscopically (data not shown). It is noteworthy that the percentage differences in B cells in $Lyn^{-/-}$ mice reflect differences in absolute B cell number, as the average numbers of nucleated cells derived from the organs of $Lyn^{+/+}$ or $Lyn^{-/-}$ mice were essentially the same (refer to Figure 2 legend).

The reduction in B cell numbers was not due to a selective block in B cell development, as the proportion of peripheral B cells expressing B cell developmental markers, such as major histocompatibility complex class II, surface IgD, CD23, heat stable antigen, and MEL14 (data not shown), was the same in $Lyn^{-/-}$ and control mice.

No significant differences in the T cell composition of both primary and secondary lymphoid tissues from $Lyn^{-/-}$ mice were noted (Figure 2B; data not shown); T cell subsets in the thymus were normal (data not shown). In secondary lymphoid tissue, there was a slight increase in the proportion of T cells, probably as a direct result of a corresponding decrease in B cells in the same tissue (Figure 2B).

B Cell Function Is Impaired in $Lyn^{-/-}$ Mice

The reduction in numbers of recirculating B cells in $Lyn^{-/-}$ mice suggests a defect in their ability to either proliferate or persist in the periphery. To distinguish between these possibilities, we measured the proliferative potential of B cells derived from the axillary lymph node, mesentric lymph node, or spleen in a tritium incorporation assay following stimulation of cultures with either LPS or anti-immunoglobulin (Figure 3A). Axillary lymph nodes showed little difference between $Lyn^{+/+}$ and $Lyn^{-/-}$ mice in B cell number, while differences in B cell numbers between spleen and mesenteric lymph node were 2-fold and 3-fold, respectively (see Figure 2B). To compensate for these differences, cultures were adjusted to contain equivalent numbers of B cells. While lymph node (Figure 3A) and splenic B cells (data not shown) from control mice responded typically to cross-linking of surface immunoglobulin with anti-μ, the corresponding cells from $Lyn^{-/-}$ mice responded poorly (Figure 3A), and no alteration in the kinetics of the response was evident (data not shown).

The signaling pathway linked to surface immunoglobulin appears to be distinct from that involving LPS activation, as anti-μ-induced B cell proliferation has been shown to

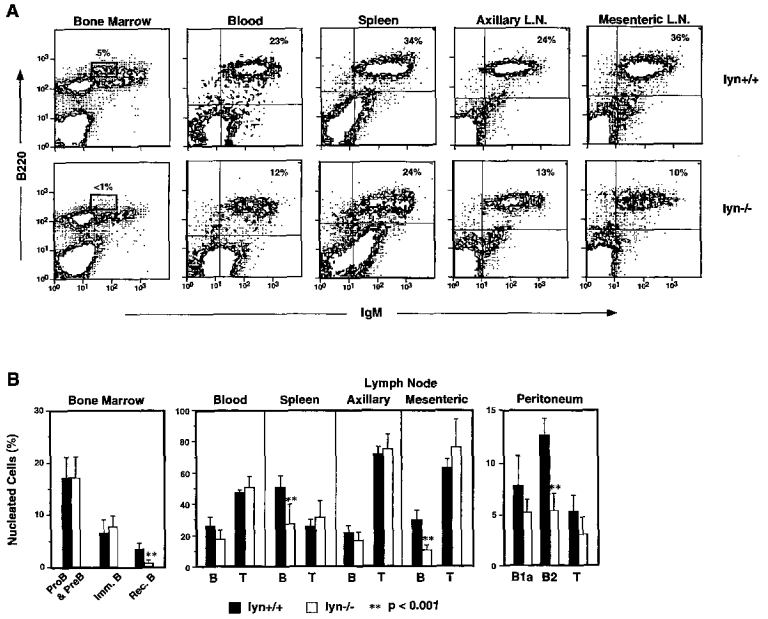

Figure 2. $Lyn^{-/-}$ Mice Have Lower Levels of Recirculating B Cells

(A) Representative two-color fluorescence analysis of lymphoid tissues from $Lyn^{+/+}$ and $Lyn^{-/-}$ mice stained using MAbs to B220 and IgM. The boxes in the bone marrow profiles show the percent of recirculating B cells; the percent of B cells present in other tissues are indicated.

(B, left) Proportion of pro-B and pre-B (proB and preB), immature B (Imm. B), and recirculating B (Rec. B) cells in the marrows of $Lyn^{+/+}$ mice (closed bars) and $Lyn^{-/-}$ mice (open bars). Results are derived from the analysis of marrows from eight mice by two-color fluorescence using MAbs to B220 and IgM. The average number of nucleated cells recovered from $Lyn^{+/+}$ and $Lyn^{-/-}$ marrows were $1.95 \times 10^7 \pm 0.3 \times 10^7$ and $2 \times 10^7 \pm 0.4 \times 10^7$, respectively.

(B, middle) Proportion of B and T cells in lymphoid tissues from $Lyn^{+/+}$ mice (closed bars) and $Lyn^{-/-}$ mice (open bars) enumerated using MAbs to B220 and CD5, respectively. Numbers of mice used in the analysis: blood (4), spleen (16), axillary lymph node (10), mesenteric lymph node (16). The average number of nucleated cells recovered from $Lyn^{+/+}$ and $Lyn^{-/-}$ mice were as follows: blood, $Lyn^{+/+}$ $8.7 \times 10^6 \pm 0.6 \times 10^6$, $Lyn^{-/-}$ $7 \times 10^6 \pm 0.4 \times 10^6$; spleen, $Lyn^{+/+}$ $1.5 \times 10^8 \pm 0.3 \times 10^8$, $Lyn^{-/-}$ $1.2 \times 10^8 \pm 0.1 \times 10^8$; axillary lymph node, $Lyn^{+/+}$ $10^7 \pm 0.3 \times 10^7$, $Lyn^{-/-}$ $1.3 \times 10^7 \pm 0.45 \times 10^7$; mesenteric lymph node, $Lyn^{+/+}$ $2.8 \times 10^7 \pm 0.4 \times 10^7$ $Lyn^{-/-}$ $2.4 \times 10^7 \pm 0.8 \times 10^7$.

(B, right) Proportion of Ly-1$^+$ B cells (B1a), conventional B cells (B2) and T cells (T) in the peritoneal cavity of $Lyn^{+/+}$ mice (closed bars) and $Lyn^{-/-}$ mice (open bars). Results are derived from the analysis of peritoneal cells from five mice by three-color fluorescence using MAbs to B220, CD5, and IgD. The average number of nucleated cells recovered from $Lyn^{+/+}$ and $Lyn^{-/-}$ peritoneum were $5.4 \times 10^6 \pm 2.2 \times 10^6$ and $7.3 \times 10^6 \pm 2.7 \times 10^6$ respectively.

Asterisks indicate statistical significance, $p < 0.001$ using Student's t test. Data are represented as mean ± SD.

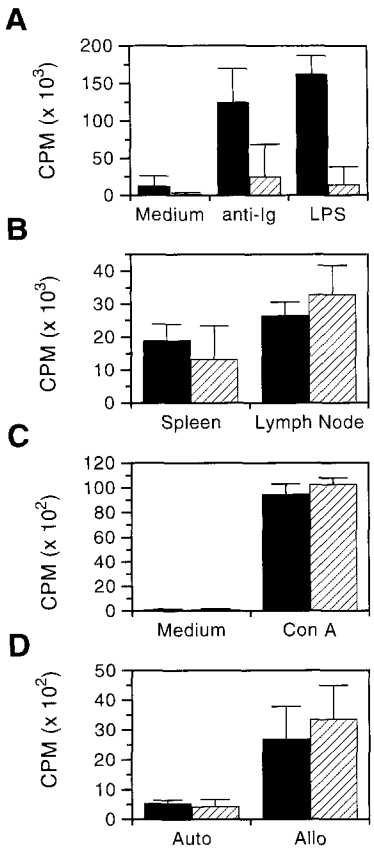

Figure 3. B and T Cell Function in $Lyn^{-/-}$ Mice

(A) Mesenteric lymph node cells from $Lyn^{+/+}$ (closed bars) or $Lyn^{-/-}$ mice (hatched bars) were cultured for 3 days in the presence of medium, LPS, or anti-μ. DNA synthesis was measured by pulsing with [^{3}H]thymidine for 6 hr. Representative result of one out of six experiments is shown.

(B) Lymph node and spleen cells from $Lyn^{+/+}$ (closed bars) or $Lyn^{-/-}$ mice (hatched bars) were cultured on mitotically inactivated fibroblasts expressing CD40 ligand for 3 days. Cultures were pulsed with [^{3}H]thymidine for 6 hr. Representative result of one out of three experiments is shown.

(C) Mesenteric lymph node cells from $Lyn^{+/+}$ (closed bars) or $Lyn^{-/-}$ mice (hatched bars) were cultured for 3 days in the presence of medium or the T cell mitogen concanavalin A. DNA synthesis was measured by pulsing with [^{3}H]thymidine for 6 hr. Representative result of one out of three experiments is shown.

(D) One-way MLR using mitotically inactivated stimulator spleen cells from either BALB/c allogeneic mice (allo MLR) or syngeneic mice (auto MLR). Responder cells were derived from lymph nodes of $Lyn^{+/+}$ (closed bars) or $Lyn^{-/-}$ mice (hatched bars). Data are represented as mean ± SD. Representative result of one out of two experiments is shown.

require CD45 (Kishihara et al., 1993) and VAV (Tarakhovsky et al., 1995; Zhang et al., 1995) expression, while LPS activation is independent of both. To determine the relative response to LPS, equivalent numbers of lymph node (Figure 3A) and splenic B cells (data not shown) from $Lyn^{+/+}$ and $Lyn^{-/-}$ mice were assessed for their ability to respond to LPS treatment. While B cells from control animals showed a typical response, with a peak at 3 days, B cells from $Lyn^{-/-}$ mice responded poorly (Figure 3A). These data indicate that LYN is an important component of the BCR complex and plays an indispensable role in normal B cell proliferation.

Interactions between CD40 and its ligand are pivotal in T-dependent (TD) B cell antibody responses (Banchereau et al., 1994). A recent study has shown that LYN is rapidly activated upon cross-linking of CD40 (Ren et al., 1994). To address whether B cells from $Lyn^{-/-}$ mice could respond to stimulation through CD40, spleen and axillary lymph node cells from $Lyn^{-/-}$ and control mice were plated on mitotically inactivated NIH 3T3 fibroblasts constitutively expressing mouse CD40 ligand. No difference was observed in the proliferative potential of splenic or lymph node–derived B cells from control or $Lyn^{-/-}$ mice, demonstrating that LYN is not crucial for signaling a CD40-mediated proliferative response (Figure 3B).

Although LYN is not expressed in normal T cells, the function of $Lyn^{-/-}$ T cells was investigated to ensure that the aberrant B cell behavior in the $Lyn^{-/-}$ mice was not a consequence of impaired T cell function. No difference in proliferation in the presence of the T cell mitogen concanavalin A was observed in lymph node T cells from $Lyn^{+/+}$ and $Lyn^{-/-}$ mice (Figure 3C). Moreover, T cells from $Lyn^{+/+}$ and $Lyn^{-/-}$ mice, in one-way mixed lymphocyte reactions (MLR) using either autologous or allogeneic stimulator cells, were indistinguishable in their response (Figure 3D).

$Lyn^{-/-}$ Mice Have Elevated Levels of Serum IgM

The levels of immunoglobulin isotypes in the serum were measured by enzyme-linked immunosorbent assay (ELISA). $Lyn^{-/-}$ mice showed normal levels of circulating IgG1, IgG2a, IgG2b, and IgG3, but a 10-fold elevation in serum IgM (Figure 4A). $Lyn^{+/-}$ mice had a slightly higher level of IgM than $Lyn^{+/+}$ mice, but 5-fold less than $Lyn^{-/-}$ mice (Figure 4A).

An enzyme-linked immunospot (ELISPOT) assay for detection of antibody-secreting cells was used to determine if the elevated level of circulating IgM was due to an increase in the number of antibody-forming cells (AFCs; Figure 4B). While no significant differences were observed in the number of IgG1-AFCs in $Lyn^{-/-}$ mice compared with control mice, there was a 10-fold increase in the number of IgM-AFCs in all $Lyn^{-/-}$ lymphoid tissues examined (Figure 4B). Thus, the elevated levels of circulating IgM in $Lyn^{-/-}$ animals is a result of an elevation in the total number of IgM-producing plasma cells.

Perturbed Humoral Immune Responses in $Lyn^{-/-}$ Mice

Mice challenged with T-independent (TI) antigens secrete IgM, followed by a switch to IgG3 (Coffman et al., 1993). To determine whether this response was impaired in $Lyn^{-/-}$ mice, groups of six $Lyn^{+/+}$, $Lyn^{+/-}$, and $Lyn^{-/-}$ mice were immunized with 10 μg of the hapten (4-hydroxy-3-nitrophenyl)acetyl (NP) coupled to the TI carrier LPS (NP–LPS), and their serum antibody response was measured weekly following immunization. The serum of all mice prior to immunization had measurable levels of NP-binding IgM antibodies, presumably due to high levels of circulating cross-reactive antibody (Figure 5A, i). Although $Lyn^{-/-}$ mice showed no measurable increase in the level of NP-specific

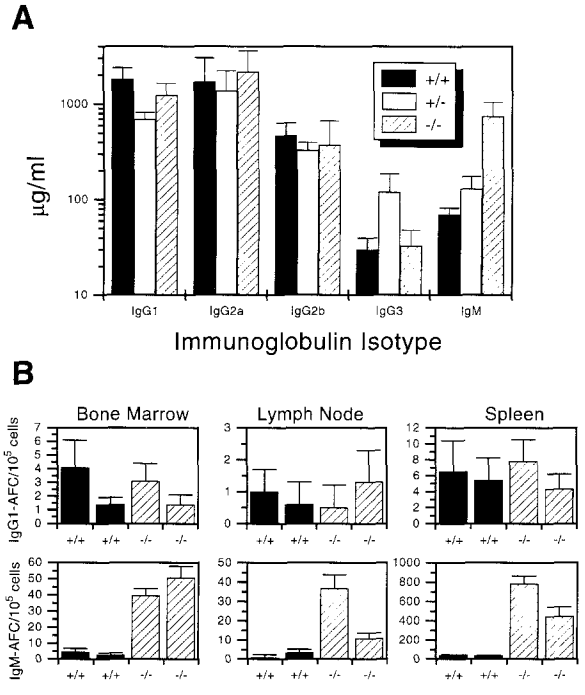

Figure 4. Levels of Immunoglobulin in the Serum of Unchallenged Mice and the Frequency of IgG1- and IgM-Secreting Cells

(A) Levels of immunoglobulin isotypes in the serum of a cohort of six $Lyn^{+/+}$ (closed bars), $Lyn^{+/-}$ (open bars), and $Lyn^{-/-}$ (hatched bars) mice as determined by ELISA. Data are represented as the geometric mean ± SD.

(B) ELISPOT was used to determine the frequency of IgG1- and IgM-AFCs in suspensions of bone marrow, mesenteric lymph node, and spleen prepared from two $Lyn^{+/+}$ (closed bars) and two $Lyn^{-/-}$ (hatched bars) mice. Data are represented as mean ± SD of eight replicate wells per sample. Representative result of one out of three experiments is shown.

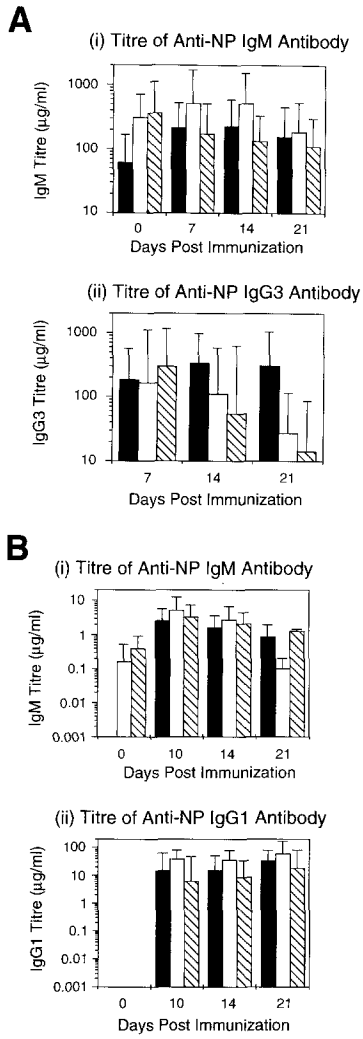

Figure 5. The Immune Response of $Lyn^{-/-}$ Mice after Challenge with TI and TD Antigens

(A) IgM (i) and IgG3 (ii) response of a cohort of $Lyn^{+/+}$ (closed bars), $Lyn^{+/-}$ (open bars), and $Lyn^{-/-}$ (hatched bars) mice at the indicated times after immunization with 10 µg of NP-LPS.

(B) IgM (i) and IgG1 (ii) response of a cohort of $Lyn^{+/+}$ (closed bars), $Lyn^{+/-}$ (open bars), and $Lyn^{-/-}$ (hatched bars) mice at the indicated times after immunization with 100 µg of NP-KLH. Data are represented as geometric mean ± SD.

IgM after immunization with NP–LPS, their ability to respond to this antigen was evidenced by the appearance of NP-specific IgG3 (Figure 5A, i and ii). While $Lyn^{-/-}$ mice mounted an efficient IgG3 response within 1 week of immunization, this response decayed more rapidly than that of control mice (Figure 5A, ii). The IgG3 response of $Lyn^{+/-}$ mice also decayed more rapidly than that of $Lyn^{+/+}$ mice, but was still greater than the response of $Lyn^{-/-}$ mice. These data indicate that $Lyn^{-/-}$ mice are incapable of sustaining normal antibody responses to TI antigens.

Challenging mice with TD antigens induces the rapid secretion of low affinity IgM antibodies followed by a switch to secretion of IgG and, following somatic mutation, secretion of higher affinity antibodies (Allen et al., 1987). To determine whether TD responses were impaired in $Lyn^{-/-}$ mice, groups of mice were immunized with 100 µg of NP coupled to the protein keyhole limpet hemocyanin (KLH). Although both $Lyn^{-/-}$ and $Lyn^{+/-}$ mice again had detectable levels of circulating cross-reactive IgM antibody prior to immunization, the titer increased after immunization in a manner analogous to control mice (Figure 5B, i). Furthermore, the three groups of mice produced NP-specific IgG1 with similar kinetics, and to a similar serum titer (Figure 5B, ii).

Histological sections of lymph nodes from $Lyn^{+/+}$ mice maintained in a conventional animal facility showed the presence of numerous germinal centers in B cell follicles (Figure 6A). By contrast, lymph nodes from littermate $Lyn^{-/-}$ mice show very poorly formed germinal centers, suggesting some defect in TD responses (Figure 6B). The number of follicle center cells was reduced, the follicles lacked zonation, and the mantle zones were poorly developed. With progressive aging, there was severe depletion of cortical lymphocytes, resulting in small atrophic lymph nodes, although plasma cells were still present within the medullary cords. Similar progressive changes were seen in the B cell zones of the splenic white pulp.

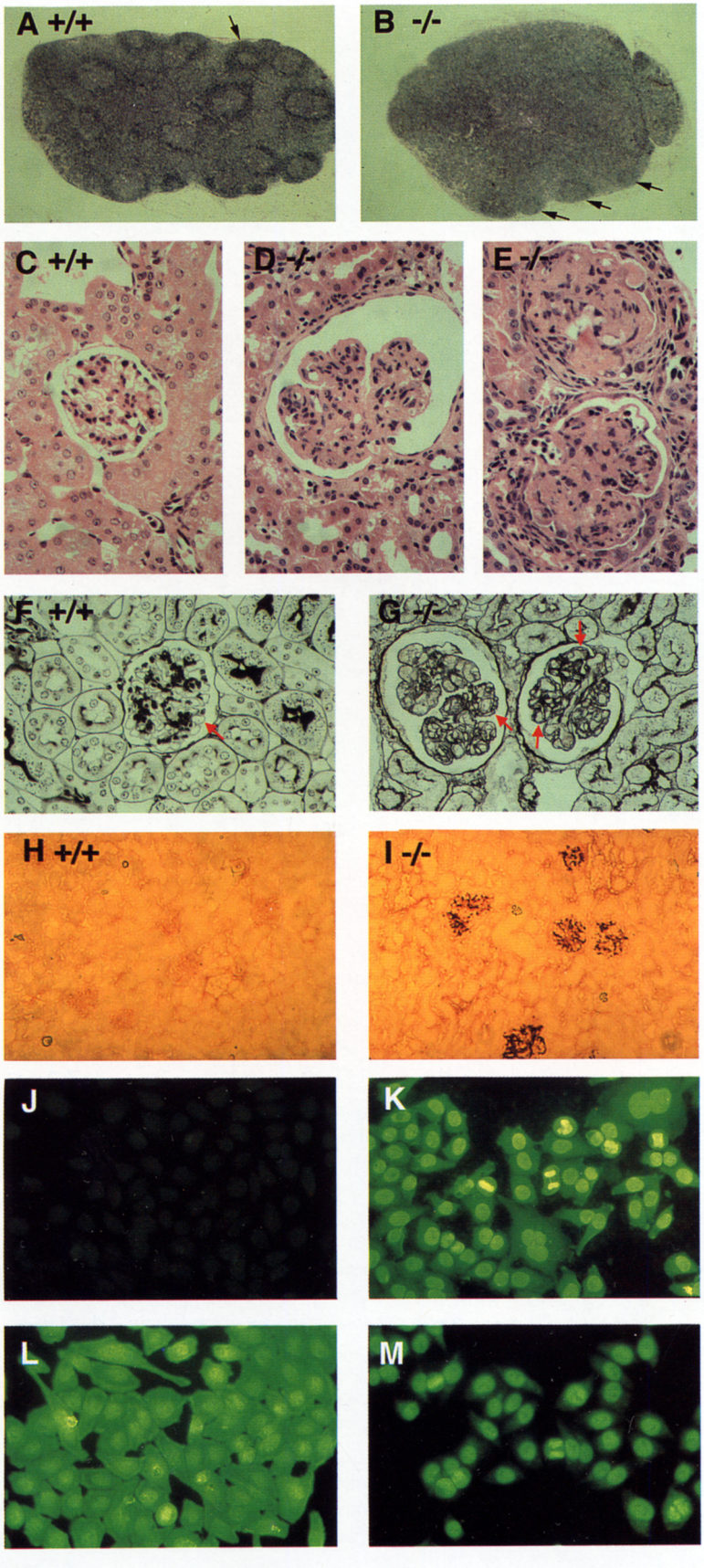

Figure 6. Lymph Node Histology, Kidney Pathology, and Autoantibodies in Control and $Lyn^{-/-}$ Mice

(A) Low power view of a lymph node from a control mouse showing well-formed secondary follicles with germinal centers (arrow).

(B) Low power view of a lymph node from a $Lyn^{-/-}$ mouse showing poorly formed follicles (indicated by arrows).

(C) High power view of the renal cortex from a control mouse showing a normal glomerulus.

(D) High power view of the renal cortex from a $Lyn^{-/-}$ mouse showing an abnormal glomerulus with hypercellularity, lobularity, and segmental sclerosis.

(E) High power view of the renal cortex from a $Lyn^{-/-}$ mouse showing severely damaged glomeruli with global sclerosis and crescent formation.

(F) High power view of PAS-M-stained section through the renal cortex of a control mouse showing normal single contour of peripheral capillary loop basement membrane.

(G) High power view of PAS-M-stained section through the renal cortex of a $Lyn^{-/-}$ mouse indicating mesangial interposition seen as tram-tracking or double contours of the peripheral capillary loop (arrows).

(H) View of the renal cortex from a control mouse stained with a pool of goat anti-mouse IgGs indicating a lack of immune complexes (magnification, 200×).

(I) View of the renal cortex from a $Lyn^{-/-}$ mouse showing IgG-containing immune complexes in glomeruli (magnification, 200×).

(J–M) Immunofluorescent analysis of human HEp-2 cells stained with antisera from a control mouse (J) and different $Lyn^{-/-}$ mice (K–M) (magnification 200×).

IgE-Mediated Anaphylaxis Is Defective in $Lyn^{-/-}$ Mice

Since LYN has been shown to be associated with the FcεRI complex and since IgE-mediated anaphylaxis is dependent on FcεRI triggering of mast cells, we sought to determine whether FcεRI triggering is compromised in $Lyn^{-/-}$ mice in a passive cutaneous anaphylaxis (PCA) model (Wershil et al., 1987). While control mice mounted a rapid PCA reaction, which is readily visualized by Evans blue extravasation due to an increase in vascular permeability as a result of mast cell degranulation, $Lyn^{-/-}$ mice failed to mediate this anaphylactic response (Figure 7). The defect reflected an impairment in mast cell function rather than simply a reduction in mast cell numbers, as no differences in the numbers of mast cells in the ears of $Lyn^{+/+}$ and $Lyn^{-/-}$ mice was noted (data not shown).

$Lyn^{-/-}$ Mice Develop Severe Glomerulonephritis as a Result of IgG Immune Complex Deposition in the Kidney

With increasing age, we noticed a significant decline in the numbers of $Lyn^{-/-}$ mice compared with control mice. Unlike control mice that remained healthy, a proportion of $Lyn^{-/-}$ mice aged from 4 weeks to 10 months became emaciated and were sacrificed. Analysis of their peripheral blood showed that all animals were severely anemic, and several were also leukopenic and thrombocytopenic (data not shown). Analysis of the bone marrows of these mice indicated that the pancytopenia was most likely due to peripheral destruction of hematopoietic cells and not to primary marrow failure (data not shown). Extramedullary hematopoiesis was notably increased within splenic tissue after 16 weeks of age.

Histological examination of solid organs revealed severe renal disease (Figure 6). Glomerular damage consisting of hypercellularity, lobularity, and focal sclerosis was apparent (Figure 6D). In some instances, glomeruli were globally sclerotic; glomerular crescents were occasionally seen (Figure 6E). In addition, mesangial interposition was present in the peripheral capillary loops (Figure 6G). Occasional animals also showed necrotic glomerular lesions, consistent with a microcapillary vasculitis. These severe glomerulonephritic changes correlate clinically with renal failure, a probable cause for the demise of some $Lyn^{-/-}$ animals. Analysis of the kidneys from apparently healthy $Lyn^{-/-}$ mice of 6 weeks of age showed variable, but less severe glomerular damage, indicating early onset of the renal disease (data not shown).

The possibility that the glomerulonephritic process was secondary to immune dysfunction was investigated. Immunochemical staining of frozen sections of kidney using isotype-specific antibodies showed deposition of IgG immune complexes in the glomeruli (Figure 6I). This immune complex deposition was evident in mice at an early age (data not shown). The presence of immune complexes was confirmed by electron microscopy, since subendothelial and mesangial electron dense deposits were identified (data not shown). Immune complex glomerulonephritis is only seen when the precipitating antigen is persistent, as in chronic infections or autoimmune disease. The presence of autoreactive antibodies was investigated by testing the capacity of sera from glomerulonephritic $Lyn^{-/-}$ and control mice to react with autoantigens. While no staining was seen using serum from control mice (Figure 6J), autoantibodies were evident in serum from glomerulonephritic $Lyn^{-/-}$ mice (Figures 6K–6M). While most sera reacted with nuclear and cytoplasmic antigens (Figures 6K and 6L), some reacted predominantly with nuclear antigens (Figure 6M). Collectively, these data indicate that the glomerulonephritis seen in $Lyn^{-/-}$ mice is due to the deposition of IgG immune complexes containing autoreactive antibodies.

A survival study has shown that by 25 weeks of age, 42% of $Lyn^{-/-}$ mice had either succumbed or were developing signs of autoimmune disease, as evidenced by the presence of blood in their urine. Moreover, >90% of mice of more than 6 weeks of age showed histological signs of autoimmune disease.

Figure 7. Passive Cutaneous Anaphylaxis in Control and $Lyn^{-/-}$ Mice

$Lyn^{+/+}$ (left of figure) and $Lyn^{-/-}$ mice (right of figure) were given intradermal injections in their left ears with 20 ng of mouse anti-DNP IgE diluted in PBS and in their right ears with PBS. After 24 hr, mice were injected intravenously with DNP–HSA in Evans blue. The typical PCA reaction, as indicated by extravasation of Evans blue dye, is seen in the left ear of the $Lyn^{+/+}$ mouse but is not evident in the corresponding ear of the $Lyn^{-/-}$ mouse.

Discussion

Our studies of $Lyn^{-/-}$ mice have revealed that LYN has an indispensable role in BCR-mediated signal transduction that is required for T cell–independent B cell proliferation and in triggering the elimination of autoreactive B cells.

All $Lyn^{-/-}$ mice have reduced numbers of B cells, although different lymphoid tissues from the same mouse show considerable variation. The peritoneal cavity, mesenteric lymph nodes, and Peyer's patches, which perhaps resemble the most active lymphoid compartments, show the greatest depletion in B cells. A reduction in bone marrow output might explain the peripheral B cell deficit; however, there is no evidence to suggest any alterations in B cell developmental compartments in $Lyn^{-/-}$ marrows. While it is also feasible that the longevity of peripheral B cells may be reduced, the more probable explanation for the reduction in B cell numbers in $Lyn^{-/-}$ mice is a failure

of B cells to expand in the periphery. This explanation is consistent with our in vitro studies for B cell proliferation and is implied from both the histological examination of lymph nodes, which show a failure to form normal germinal centers, and the reduced duration of the TI response in $Lyn^{-/-}$ mice.

Germinal centers develop in B cell follicles of secondary lymphoid tissues during TD antibody responses and are associated with clonal B cell expansion, somatic mutation of immunoglobulin variable region genes, and selection of higher affinity antibodies, as well as the generation of plasma cells and memory B cells (MacLennan, 1994). Thus, the apparent failure of $Lyn^{-/-}$ mice to develop normal germinal centers suggests that there may be defects in some aspects of TD responses such as the ability to generate high affinity antibodies or memory B cells. This phenomenon, however, may depend on antigen concentration, since in preliminary experiments $Lyn^{-/-}$ mice showed an impairment in their primary TD response only at low doses of antigen (data not shown). The absence of normal germinal centers and elevated levels of serum IgM found in $Lyn^{-/-}$ mice is also seen in humans carrying a mutation in the gene encoding CD40 ligand (Aruffo et al., 1993). That the absence of normal germinal centers in $Lyn^{-/-}$ mice is not due to a defect in CD40 signaling is indicated by two observations. First, $Lyn^{-/-}$ mice have normal IgG serum titers and generate IgG1 antibodies in response to a TD antigen, whereas the CD40 ligand mutation results in agammaglobulinemia (Aruffo et al., 1993). Second, $Lyn^{-/-}$ B cells proliferate normally when stimulated through CD40.

B cell abnormalities associated with $Lyn^{-/-}$ mice resemble those seen in mice carrying either naturally occurring or engineered mutations in other genes. The *xid* mouse is characterized by a mutation in BTK (Thomas et al., 1993; Rawlings et al., 1993). As in $Lyn^{-/-}$ mice, *xid* mice have reduced numbers of peripheral B cells and show poor proliferation in response to stimulation with anti-immunoglobulin and possibly also LPS (Belmont, 1995). Additionally, TD antibody responses in *xid* mice are essentially normal, and TI responses are severely impaired (Belmont, 1995). The two phenotypes, however, are not identical; B cell deficiency in *xid* mice is due to a maturational block, and *xid* mice show reduced levels of serum IgM. Despite these differences, the similarity between the $Lyn^{-/-}$ and *xid* phenotypes is intriguing, and it is tempting to speculate that BTK and LYN participate in the same signal transduction pathways.

It is noteworthy that $Oct\text{-}2^{-/-}$ mice, like $Lyn^{-/-}$ mice, have reduced numbers of recirculating B cells, and in addition, $Oct\text{-}2^{-/-}$ B cells fail to respond to TI mitogens but proliferate and differentiate normally in response to T cell signals in vitro (Corcoran et al., 1993; Corcoran and Karvelas, 1994). Immune responses to TI antigens in mice repopulated with $Oct\text{-}2^{-/-}$ cells are also depressed. Oct-2, however, does not regulate *Lyn* gene transcription, as normal levels of *Lyn* message are present in $Oct\text{-}2^{-/-}$ B cells (Corcoran and Karvelas, 1994). Finally, the phenotype of $Vav^{-/-}$ mice shows a number of similarities to $Lyn^{-/-}$ mice. $Vav^{-/-}$ mice show diminished B cell responses to anti-immunoglobulin, although they respond normally to LPS (Tarakhovsky et al., 1995; Zhang et al., 1995) and may have reduced numbers of peripheral B cells (Tarakhovsky et al., 1995; Fischer et al., 1995). TD responses of $Vav^{-/-}$ mice also appear to be normal (Tarakhovsky et al., 1995; Zhang et al., 1995). The similarity of the B cell phenotype of mice with mutations in different signal transduction molecules is consistent with the cascade of interactions believed to occur following ligation of the BCR (Pleiman et al., 1994b).

Two aspects of the phenotype of $Lyn^{-/-}$ mice are particularly intriguing: the elevated levels of both IgM antibody and IgM-secreting cells and the existence of circulating autoantibodies. While examples of hyper-IgM with an associated autoimmunity have been described in other strains of mice, the nature of these conditions appears to be distinct from that found in $Lyn^{-/-}$ mice. In NZB and related strains, the hyper-IgM and autoantibody production are associated with a B cell hyperplasia, particularly of the Ly-1 B cell subset (Hayakawa et al., 1983). Similarly, viable motheaten mice, which are affected by a severe autoimmune condition early in life, contain only Ly-1 B cells (Sidman et al., 1986). In contrast, the Ly-1 B cell subset is unchanged in $Lyn^{-/-}$ mice. This suggests that the autoimmunity in $Lyn^{-/-}$ mice is not a consequence of changing the cellular composition of the B cell population, but rather results from altering signal transduction within each B cell. In this scheme, the differentiation of $Lyn^{-/-}$ B cells into antibody-secreting cells results from aberrant processing of an immunoglobulin-mediated signal. It is possible that, upon encountering self-antigens, $Lyn^{-/-}$ B cells are neither deleted nor do they remain ignorant, but rather differentiate into plasma cells. While self-reactive IgM antibodies are usually considered relatively benign, they could assume pathological significance at high concentration. The immune complexes generated could act as a focal point for T cell recruitment and the consequent development of a more pathological IgG-mediated condition. The glomerulonephritis and pancytopenia seen in these mice bear many similarities to the renal and hematological pathology manifest in systemic lupus erythematosus (SLE), a disease characterized by the production of multiple autoantibodies and immune complex deposition. In SLE, genetic susceptibility combined with an environmental trigger is thought to cause autoantibody production by B cells, at least in part due to abnormal B cell signaling (Mountz et al., 1991; Drake and Kotzin, 1992). Perhaps the normal function of LYN is critical for the maintenance of self-tolerance in the face of adverse environmental triggers.

In addition to the importance of LYN in B cell signaling, our studies have also pointed to a critical role for LYN in mast cell function. The importance of FcεRI in the allergic response has previously been demonstrated in mice lacking this receptor by disruption of either α or γ subunits (Dombrowicz et al., 1993; Takai et al., 1994). We have shown that mice deficient in a signal transduction molecule, LYN, are defective in mediating cutaneous anaphylaxis and thus directly implicate LYN as a crucial signaling component of this receptor complex.

B cells can respond in a number of different ways to stimulation with antigen, and their response is dependent

on their state of differentiation and on the concentration of antigen. They can be induced to proliferate, to differentiate into antibody producing cells or memory cells, and under certain conditions, they can be either clonally deleted or made unresponsive. Our data suggests that LYN is not only necessary for B cell proliferation but also for clonal deletion of autoreactive B cells. Future studies will be aimed at investigating the role of LYN in establishing B cell tolerance.

Experimental Procedures

Generation of *Lyn*$^{-/-}$ Mice

Genomic clones containing the mouse *Lyn* promoter were used to construct the targeting vector and have been described previously (Hibbs et al., 1995). The PGKNeo expression cassette (Tybulewicz et al., 1991) was inserted in reverse transcriptional orientation to the *Lyn* gene between a PstI site upstream of the promoter and an XbaI site approximately 11.5 kb downstream in intron 1, creating a construct with a long arm of homology of 5.3 kb and a short arm of 1.1 kb in length.

E14 ES cells (Handyside et al., 1989) were propagated and electroporated as described (Mann et al., 1993). Selection for growth in G418 was initiated 24 hr after electroporation, and G418-resistant colonies were micromanipulated after a further 7 days. We replated 20% of the cells comprising an individual colony into a well of a 96-well plate containing mitotically inactivated STO cells and used these as a stock; the remaining 80% of cells were replated and cultured for a further 4 days, after which DNA was prepared from pools of two or four clones. PCR reactions were carried out using 1 μl of the DNA sample in the presence of 2.0 mM $MgCl_2$ using *Tth plus* DNA polymerase (Biotec International, Bentley, Western Australia). PCR products were generated by 35 cycles at 95°C (30 s), 60°C (30 s), and 72°C (90 s). Of the primers used to identify homologous recombinants, primer 1 was complementary to sequences at the 5′ end of the PGK promoter (5′-dTGCTACTTCCATTTGTCACGTCC-3′), and primer 2 was complementary to *Lyn* genomic sequences downstream of the short arm of homology (5′-dACAGAGCTAGACCGTTCTTTCCTC-3′) (Figure 1A). A third primer was used in combination with primer 2 to identify the wild-type *Lyn* allele (5′-dCAGGTGGAGCATACCTGGCTGTTT-3′).

Two targeted ES cell clones identified by PCR, and verified by Southern blot analysis, were injected into blastocysts of C57BL/6 mice and transplanted into the uteri of psuedopregnant females. Chimeric animals were mated with C57BL/6 mice, and germline transmission of the mutated *Lyn* allele was identifed by Southern blot analysis of NcoI-digested genomic DNA using probes to *Lyn* genomic sequences outside of the targeting vector (Figure 1A) and to the *neo*^{r} gene. Mice were maintained in a conventional animal facility.

Immunoprecipitation and Kinase Assays

Spleen and liver extracts were prepared, immunoprecipitated with preimmune or LYN-specific antisera, and subject to kinase assay as described (Stanley et al., 1991).

Flow Cytometric Analysis

Bone marrow cells were obtained by flushing femurs, and peritoneal cavity cells were isolated by peritoneal lavage using PBS, 1% FBS. Peripheral blood (0.2 ml) was depleted of red blood cells using 0.83% NH_4Cl prior to staining. Single cell suspensions were prepared from lymphoid organs in PBS, 1% FBS. Cells (10^5) were incubated with FITC- and PE-conjugated MAbs and analyzed using a FACScan (Becton-Dickinson, San Jose, CA). For three-color analysis, a biotinylated antibody revealed with TriColor Avidin (Caltag, South San Francisco, CA) was used in addition to direct FITC and PE conjugates. Dead cells were excluded on the basis of propidium iodide uptake, and 10,000 events were acquired. The following MAbs were used: RA3-6B2 (B220), 331.12 (IgM), goat anti-mouse IgD (Nordic Immunological Laboratories, Tilburg, The Netherlands), 187.1 (Igκ), JC5 (Igλ), S7 (CD43), B3B4 (CD23), M1/69 (HSA), M5/114 ($Ia^{b,d}$), GK1.5 (CD4), 53.6 (CD8), 53.7 (CD5), M1/70 (CD11b), 6B2-8C5 (GR-1), and MEL14 (L-selectin).

Proliferation Assays

Cells were cultured at a density of 5×10^5 B cells/ml in complete RPMI. Anti-immunoglobulin stimulation was performed using a $F(ab')_2$ goat anti-mouse IgM (Capella, Durham, NC) at a final concentration of 25 μg/ml. LPS (Difco, Detroit, MI) was used at a final concentration of 20 μg/ml. CD40 ligand–transfected 3T3 fibroblasts were generated using standard techniques and were irradiated at 3000 rad. Tritiated thymidine (10 μCi) was added to the cultures on the indicated days, and the cells were harvested 6 hr later. DNA was immobilized onto filters, and the amount of thymidine incorporated was determined using a scintillation counter (Packard Instrument Company, Meriden, CT).

Immunization, ELISA, and ELISPOT Assays

NP–KLH (100 μg in alum) and NP–LPS (10 μg in PBS), prepared as described (Lalor et al., 1992), were administered by intraperitoneal injection. Serum titers of antigen-specific immunoglobulin of the indicated isotypes were determined at regular intervals after immunization using an NP-specific ELISA performed as described (Smith et al., 1994). Total serum immunoglobulin titers were determined by ELISA, using sheep anti-mouse immunoglobulin (Silenus Laboratories, Hawthorn, Australia) as a capture reagent, and developed with isotype-specific goat sera directly conjugated with horseradish peroxidase (Southern Biotechnology Associates Incorporated, Birmingham, AL). Purified myeloma proteins (Sigma Chemical Company, St. Louis, MO) were used as standards. ELISPOT assays were carried out as described (Lalor et al., 1992), again using sheep anti-mouse immunoglobulin (Silenus) capture and goat anti-mouse immunoglobulin (Southern Biothechnology Associates Incorporated) developing reagents.

Immunohistochemistry and Immunofluorescence

Anti-nuclear antibodies were detected using fixed human HEp-2 cells (Immuno-Concepts, Sacramento, CA), following the instructions of the manufacturer. Sera from *Lyn*$^{+/+}$ and *Lyn*$^{-/-}$ mice were used at a dilution of 1:100 and 1:1000, respectively. Bound antibodies were revealed with a fluoresceinated sheep anti-mouse immunoglobulin serum (Silenus Laboratories). Frozen sections of kidneys were prepared and stained as described (Smith et al., 1994). Immune complexes were detected by staining with a pool of IgG1-, IgG2a-, and IgG2b-specific sera directly conjugated to horseradish peroxidase (Southern Biotechnology Associates Incorporated).

Histology

Tissues were fixed for light microscopy in either formalin or Bouin's solution for 24 hr and embedded in paraffin. Sections were stained with hematoxylin and eosin, periodic acid silver methananine (PAS-M), or alcian blue according to standard procedures. Sections for electron microscopy were prepared following fixation in 2.5% glutaraldehyde, postfixing in osmium tetroxide, embedding in Spurr's resin, and staining with lead citrate.

Passive Cutaneous Anaphylaxis

Control and *Lyn*$^{-/-}$ mice were anaesthetized with chloral hydrate and then given intradermal injections of 20 ng of mouse anti-DNP IgE antibody (Sigma) diluted in 20 μl of PBS in their left ears. The right ears of the same mice were injected with PBS. After 24 hr, the mice were given an intravenous injection of 100 μg of DNP–HSA (Sigma) in 100 μl of 0.9% NaCl, 1% Evans blue dye. The PCA reaction was evident within 5 min of the second injection, and after 60 min, mice were culled and their ears subject to histological analyses.

Acknowledgments

The authors would like to thank A. Burgess for comments on the manuscript. We are grateful to M. Inglese for blastocyst injections, W. Angel and J. Merryfull for their tireless work in the Animal Facility, V. Feakes for histology preparation, M. McLean and A. Light for assistance with ELISAs and cell cultures, and L. Cox and J. Strickland for photography. M. L. H. was supported by a Queen Elizabeth II fellowship from the Australian Research Council and D. M. T. by a fellowship from the National Health and Medical Research Council of Australia and grant A1-03958 from the National Institute of Allergy and Infectious Diseases.

Received July 3, 1995; revised September 11, 1995.

References

Allen, D., Cumano, A., Dildrop, R., Kochs, C., Rajewsky, K., Rajewsky, N., Roes, J., Sablitzky, F., and Siekevitz, M. (1987). Timing, genetic requirements and functional consequences of somatic hypermutation during B-cell development. Immunol. Rev. *96*, 5–22.

Aruffo, A., Farrington, M., Hollenbaugh, D., Li, X., Milatovich, A., Nonoyama, S., Bajorath, J., Grosmaire, L.S., Stenkamp, R., Neubauer, M., Roberts, R.L., Noelle, R.J., Ledbetter, J.A., Francke, U., and Ochs, H.D. (1993). The CD40 ligand, gp39, is defective in activated T cells from patients with X-linked hyper-IgM syndrome. Cell *72*, 291–300.

Banchereau, J., Bazan, F., Blanchard, D., Briere, F., Galizzi, J.P., van Kooten, C., Liu, Y.J., Rousset, F., and Saeland, S. (1994). The CD40 antigen and its ligand. Annu. Rev. Immunol. *12*, 881–922.

Belmont, J.W. (1995). Insights into lymphocyte development from X-linked immune deficiencies. Trends Genet. *11*, 112–116.

Blank, U., Ra, C., Miller, L., White, K., Metzger, H., and Kinet, J.-P. (1989). Complete structure and expression in transfected cells of high affinity IgE receptor. Nature *337*, 187–189.

Bolen, J.B., Rowley, R.B., Spana, C., and Tsygankov, A.Y. (1992). The src family of tyrosine protein kinases in hemopoietic signal transduction. FASEB J. *6*, 3403–3409.

Burkhardt, A.L., Brunswick, M., Bolen, J.B., and Mond, J.J. (1991). Anti-immunoglobulin stimulation of B lymphocytes activates src-related protein-tyrosine kinases. Proc. Natl. Acad. Sci. USA *88*, 7410–7414.

Campbell, M.-A., and Sefton, B.M. (1990). Protein tyrosine phosphorylation is induced in murine B lymphocytes in response to stimulation with anti-immunoglobulin. EMBO *9*, 2125–2131.

Campbell, M.-A., and Sefton, B.M. (1992). Association between B-lymphocyte membrane immunoglobulin and multiple members of the src family of protein tyrosine kinases. Mol. Cell. Biol. *12*, 2315–2321.

Clark, M.R., Campbell, K.S., Kazlauskas, A., Johnson, S.A., Hertz, M., Potter, T.A., Pleiman, C., and Cambier, J.C. (1992). The B cell antigen receptor complex: association of Ig-α and Ig-β with distinct cytoplasmic effectors. Science *258*, 123–126.

Coffman, R.L., Lebman, D.A., and Rothman, P. (1993). Mechanism and regulation of immunoglobulin isotype switching. Adv. Immunol. *54*, 229–270.

Corcoran, L.M., and Karvelas, M. (1994). Oct-2 is required early in T cell-independent B cell activation for G1 progression and for proliferation. Immunity *1*, 635–645.

Corcoran, L.M., Karvelas, M., Nossal, G.J.V., Ye, Z.-S., Jacks, T., and Baltimore, D. (1993). Oct-2, although not required for early B-cell development, is critical for later B-cell maturation and for postnatal survival. Genes Dev. *7*, 570–582.

Corey, S.J., Burkhardt, A.L., Bolen, J.B., Geahlen, R.L., Tkatch, L.S., and Tweardy, D.J. (1994). Granulocyte colony-stimulating factor receptor signaling involves the formation of a three-component complex with Lyn and Syk protein-tyrosine kinases. Proc. Natl. Acad. Sci. USA *91*, 4683–4687.

Dombrowicz, D., Flamand, V., Brigman, K.K., Koller, B.H., and Kinet, J.-P. (1993). Abolition of anaphylaxis by targeted disruption of the high affinity immunoglobulin E receptor α chain gene. Cell *75*, 969–976.

Drake, C.G., and Kotzin, B.L. (1992). Genetic and immunological mechanisms in the pathogenesis of SLE. Curr. Opin. Immunol. *4*, 733–740.

Eiseman, E., and Bolen, J.B. (1992). Engagement of the high-affinity IgE receptor activates *src* protein–related tyrosine kinases. Nature *355*, 78–80.

Fischer, K.-D., Zmuidzinas, A., Gardner, S., Barbacid, M., Bernstein, A., and Guidos, C. (1995). Defective T-cell receptor signalling and positive selection of Vav-deficient $CD4^+$ $CD8^+$ thymocytes. Nature *374*, 474–476.

Gold, M.R., Law, D., and DeFranco, A.L. (1990). Stimulation of protein tyrosine phosphorylation by the B-lymphocyte antigen receptor. Nature *345*, 810–813.

Gold, M.R., Matsuuchi, L., Kelly, R.B., and DeFranco, A.L. (1991). Tyrosine phosphorylation of components of the B-cell antigen receptors following receptor crosslinking. Proc. Natl. Acad. Sci. USA *88*, 3436–3440.

Handyside, A.H., O'Neil, G.T., Jones, M., and Hooper, M.L. (1989). Use of BRL-conditioned media in combination with feeder layers to isolate a diploid embryonal stem cell line. Roux's Arch. Dev. Biol. *198*, 8–55.

Hayakawa, K., Hardy, R.R., Parks, D.R., and Herzenberg, L.A. (1983). The "Ly-1B" cell subpopulation in normal, immunodefective, and autoimmune mice. J. Exp. Med. *157*, 202–218.

Hibbs, M.L., Stanley, E., Maglitto, R., and Dunn, A.R. (1995). Identification of a duplication of the mouse *Lyn* gene. Gene *156*, 175–181.

Kishihara, K., Penninger, J., Wallace, V.A., Kundig, T.M., Kawai, K., Wakeham, A., Timms, E., Pfeffer, K., Ohashi, P.S., Thomas, M.L., Furlonger, C., Paige, C.J., and Mak, T.W. (1993). Normal B lymphocyte development but impaired T cell maturation in CD45-exon 6 protein tyrosine phosphatase-deficient mice. Cell *74*, 143–156.

Lalor, P.A., Nossal, G.J.V., Sanderson, R.D., and McHeyzer-Williams, M.G. (1992). Functional and molecular characterization of single, (4-hydroxy-3-nitrophenyl)acetyl (NP)-specific $IgG1^+$ B cells from antibody-secreting and memory B cell pathways in the C57BL/6 immune response to NP. Eur. J. Immunol. *22*, 3001–3011.

MacLennan, I.C.M. (1994). Germinal centers. Annu. Rev. Immunol. *12*, 117–139.

Mann, G.B., Fowler, K.J., Gabriel, A., Nice, E.C., Williams, R.L., and Dunn, A.R. (1993). Mice with a null mutation of the TGFα gene have abnormal skin architecture, wavy hair, and curly whiskers and often develop corneal inflammation. Cell *73*, 249–261.

Mountz, J.D., Gause, W.C., and Jonsson, R. (1991). Murine models for systemic lupus erythematosus and Sjogren's syndrome. Curr. Opin. Rheumatol. *3*, 738–756.

Pleiman, C.M., Abrams, C., Gauen, L.T., Bedzyk, W., Jongstra, J., Shaw, A.S., and Cambier, J.C. (1994a). Distinct $p53/p56^{lyn}$ and $P59^{lyn8}$ domains associate with nonphosphorylated and phosphorylated Ig-α. Proc. Natl. Acad. Sci. USA *91*, 4268–4272.

Pleiman, C.M., D'Ambrosio, D., and Cambier, J.C (1994b). The B-cell antigen receptor complex: structure and signal transduction. Immunol. Today *15*, 393–399.

Ravetch, J.V. (1994). Fc receptors: rubor redux. Cell *78*, 553–560.

Rawlings, D.J., Saffran, D.C., Tsukada, S., Largaespada, D.A., Grimaldi, J.C., Cohen, L., Mohr, R.N., Bazan, J.F., Howard, M., Copeland, N.G., Jenkins, N.A., and Witte, O.N. (1993). Mutation of unique region of Bruton's tyrosine kinase in immunodeficient XID mice. Science *261*, 358–361.

Ren, C.L., Morio, T., Fu, S.M., and Geha, R.S. (1994). Signal transduction via CD40 involves activation of *lyn* kinase and phosphatidylinositol-3-kinase, and phosphorylation of phospholipase Cγ2. J. Exp. Med. *179*, 673–680.

Reth, M. (1992). Antigen receptors on B lymphocytes. Annu. Rev. Cell Biol. *10*, 97–121.

Sidman, C.L., Schultz, L.D., Hardy, R.R., Hayakawa, K., and Herzenberg, L.A. (1986). Production of immunoglobulin isotypes by $Ly\text{-}1^+$ B cells in viable motheaten and normal mice. Science *232*, 1423–1425.

Smith, K.G.C., Weiss, U., Rajewsky, K., Nossal, G.J.V., and Tarlinton, D.M. (1994). Bcl-2 increases memory B cell recruitment but does not perturb selection in germinal centers. Immunity *1*, 803–813.

Stanley, E., Ralph, S., McEwen, S., Boulet, I., Holtzman, D.A., Lock, P., and Dunn, A.R. (1991). Alternatively spliced murine *lyn* mRNAs encode distinct proteins. Mol. Cell. Biol. *11*, 3399–3406.

Stefanova, I., Corcoran, M.L., Horak, E.M., Wahl, L.M., Bolen, J.B., and Horak, I.D. (1993). Lipopolysaccharide induces activation of CD14-associated protein tyrosine kinase $p53/p56^{lyn}$. J. Biol. Chem. *268*, 20725–20728.

Takai, T., Li, M., Sylvestre, D., Clynes, R., and Ravetch, J.V. (1994). FcR γ chain deletion results in pleiotrophic effector cell defects. Cell *76*, 519–529.

Tarakhovsky, A., Turner, M., Schaal, S., Mee, P.J., Duddy, L.P., Rajewsky, K., and Tybulewicz, V.L.J. (1995). Defective antigen receptor-mediated proliferation of B and T cells in the absence of vav. Nature *374*, 467–470.

Thomas, J.D., Sideras, P., Smith, C.I.E., Vorechovsky, I., Chapman, V., and Paul, W.E. (1993). Colocalization of X-linked agammaglobulinemia and X-linked immunodefiency genes. Science *261*, 355–358.

Tybulewicz, V.L.J., Crawford, C.E., Jackson, P.K., Bronson, R.T., and Mulligan, R.C. (1991). Neonatal lethality and lymphopenia in mice with a homozygous disruption of the c-*abl* proto-oncogene. Cell *65*, 1153–1163.

Varmus, H.E., and Lowell, C.A. (1994). Cancer genes and hematopoiesis. Blood *83*, 5–9.

Wechsler, R.J., and Monroe, J.G. (1995). *src*-family tyrosine kinase $p55^{fgr}$ is expressed in murine splenic B cells and is activated in response to antigen receptor cross-linking. J. Immunol. *154*, 3234–3244.

Wershil, B.K., Mekori, Y.A., Murakami, T., and Galli, S.J. (1987). ^{125}I-fibrin deposition in IgE-dependent immediate hypersensitivity reactions in mouse skin: demonstration of the role of mast cells using genetically mast cell-deficient mice locally reconstituted with cultured mast cells. J. Immunol. *139*, 2605–2614.

Yamanashi, Y., Kakiuchi, T., Mizuguchi, J., Yamamoto, T., and Toyoshima, K. (1991). Association of B cell antigen receptor with protein tyrosine kinase lyn. Science *251*, 192–194.

Zhang, R., Alt, F.W., Davidson, L., Orkin, S.H., and Swat, W. (1995). Defective signalling through the T- and B-cell antigen receptors in lymphoid cell lacking the vav proto-oncogene. Nature *374*, 470–473.